

# Star Cluster collisions - a formation scenario for the Extended Globular Cluster Scl-dE1 GC1

P. Assmann<sup>1</sup>  $\star$ , M.I. Wilkinson<sup>2</sup>  $\dagger$ , M. Fellhauer<sup>1</sup>  $\ddagger$ , R. Smith<sup>1</sup>  $\S$

<sup>1</sup> *Departamento de Astronomía, Universidad de Concepción, Casila 160-C, Concepción, Chile*

<sup>2</sup> *Department of Physics & Astronomy, University of Leicester, University Road, Leicester LE1 7RH, UK*

19 January 2011

## ABSTRACT

Recent observations of the dwarf elliptical galaxy Scl-dE1 (Sc22) in the Sculptor group of galaxies revealed an extended globular cluster (Scl-dE1 GC1), which exhibits an extremely large core radius of about 21.2 pc. The authors of the discovery paper speculated on whether this object could reside in its own dark matter halo and/or if it might have formed through the merging of two or more star clusters. In this paper, we present N-body simulations to explore thoroughly this particular formation scenario. We follow the merger of two star clusters within dark matter haloes of a range of masses (as well as in the absence of a dark matter halo). In order to obtain a remnant which resembles the observed extended star cluster, we find that the star formation efficiency has to be quite high (around 33 per cent) and the dark matter halo, if present at all, has to be of very low mass, i.e. raising the mass to light ratio of the object within the body of the stellar distribution by at most a factor of a few. We also find that expansion of a single star cluster following mass loss provides another viable formation path. Finally, we show that future measurements of the velocity dispersion of this system may be able to distinguish between the various scenarios we have explored.

**Key words:** galaxies: dwarfs — galaxies: star clusters — methods: N-body simulations

## 1 INTRODUCTION

The general understanding of low luminosity stellar systems is that they come in two distinct flavours. On the compact side we have the globular clusters whose properties are consistent with a purely stellar composition with no need to invoke dark matter (DM) to explain their dynamical masses (e.g. Lane et al. 2010). On the more extended side, we have the dwarf spheroidal galaxies (dSph) which have similar luminosities to globular clusters but are much more extended and show enhanced velocity dispersions. These entities are believed to be highly DM dominated, typically having estimated mass-to-light (M/L) ratios of several 10s to 100s (e.g. Mateo 1998; Walker et al. 2009), with values as high as 1000 being claimed for some of the faintest systems (e.g. Strigari et al. 2008; Kleyna et al. 2005). These high M/L values make the dSphs the most DM dominated objects known in the local universe (see e.g. Mateo 1998, for a convenient review). Between these two regions of parameter space there seems to be a clear gap (Gilmore et al. 2007) in the distribution of effective radii. This gap is visible over a wide range of absolute magnitudes, i.e. for several orders of magnitude in stellar mass.

With the discovery of the new ultra-faint galaxies around the Milky Way (see e.g. Belokurov et al. 2010, and references therein, for the latest discoveries), there seems to be a closing of the gap at very low stellar masses, which could be due to the tidal disruption of those small systems as they orbit the Milky Way. In this region, the distinction between star clusters and dwarf galaxies becomes blurred - in the absence of detailed chemical information about the stellar populations and star formation history, we can not be sure whether a particular object is a dissolving star cluster or a disrupting dwarf galaxy.

But this faint, low-mass end is not the only region of the diagram where the two distinct populations of stellar systems come closer to each other, reducing the gap between their half-light radius distributions. At the high-luminosity end, we have the population of ultra-compact dwarf (UCD) galaxies, which have masses up to  $10^8 M_\odot$  and effective radii of 20–40 pc. Their formation mechanism is still under debate. Do we see some freakish, high-mass outliers of the globular cluster mass-function (e.g. Mieske et al. 2002)? Are they the product of many star clusters, which have formed in a dense star forming region and then subsequently merged (Fellhauer & Kroupa 2002)? Or are they instead the stripped nuclei of dwarf galaxies (Bekki et al. 2001)? They clearly fall on the star cluster side of the above-mentioned gap but are more extended than typical clusters, suggesting a relation to dwarf galaxies. Further, some of them show evidence of M/L-ratios which can not be explained by simple stellar population mod-

$\star$  E-mail: passmann@astro-udec.cl

$\dagger$  miw6@astro.le.ac.uk

$\ddagger$  mfellhauer@astro-udec.cl

$\S$  rsmith@astro-udec.cl

els (Hasegan et al. 2005). The jury is still out on whether or not UCDs have a dynamically significant DM component.

Even in the ‘normal’ range of globular cluster luminosities, we now know of objects which are more extended than the regular globular cluster family. Regular globular clusters have effective radii of order a few pc. However, there is also a population of clusters with effective radii in the range 10–20 pc. We see those extended globular clusters (EGC) as ‘faint fuzzy’ star clusters in the discs of S0 galaxies (Larsen & Brodie 2000) and as Huxor objects in the Halo of M31 (Huxor et al. 2005).

Extended globular clusters were first found by Huxor et al. (2005) in M31. The authors searched for old objects in the halo of Andromeda and found objects which are similar to globular clusters in colour and luminosity, but with half-light radii of more than 30 pc. Their relative distances to the centre of M31 are between 15 and 35 kpc. Similarly, Hwang et al. (2005) found the first extended globular clusters in the halo of the Local Group dwarf irregular galaxy NGC 6822. The authors reported that the projected distances of these EGCs from the centre of NGC 6822 are close to 13 kpc, and estimated their half-light radii to be larger than 20 pc. This kind of object was previously unknown and could imply the existence of an intermediate population of objects between usual GCs and dSph galaxies. Further discoveries have been added to the original observations (Huxor et al. 2008), but, it is still unclear whether these are really a distinct population, or rather the large effective radius tail of a continuous distribution of cluster sizes.

Meanwhile, EGCs have also been found in many other galaxies. Extended globular star clusters (EGC) are clusters of stars for which the half-light radii ( $r_h$ ) exceed 8 – 10 pc. Their occurrence seems to be aleatory: they represent less than 3% of the clusters in NGC 5128 (Gomez & Woodley 2007), 9% of the Milky Way clusters (Harris 1996), and are more than 20% of the clusters in M51 (Chandar et al. 2004). Even though EGCs are usually found at large galactocentric radii, they can also be observed in dwarf galaxies (Da Costa et al. 2009). This additional dichotomy within the star cluster population is also not well understood. As in the case of UCDs, a possible scenario for their formation is again the merging of two or more star clusters, which have formed in a confined region (Brüns et al. 2009).

In this work we focus on the first EGC found in a dwarf elliptical galaxy. In the Sculptor group of galaxies, Da Costa et al. (2009) found an EGC (GC1) around the dwarf elliptical galaxy Scl-dE1 (Sc22). It has a half-light radius of 21.8 pc and an absolute magnitude of  $M_V = -6.7$ . Another reported characteristic of this EGC is that its stellar population seems to be indistinguishable from the population of the parent dwarf. By considering a king profile (King 1962) for the V-band surface brightness profile of this EGC, the authors were able to measure a core radius of 21.2 pc, a concentration index  $c = 0.65$  and a central surface brightness of  $23.1$  V mag arcsec $^{-2}$ . **Observationally, the half-light radius is defined as the projected radius at which the surface brightness has dropped to half its central value. In the theoretical literature, the term core radius is used to refer to the natural scalelength of the model under consideration, for example, the King model. It is important to note that these definitions do not, in general coincide and in real systems their temporal evolution may be qualitatively different due to processes such as mass segregation of stellar remnants with high mass-to-light ratios (see e.g. Hurley 2007; Wilkinson et al. 2003). In this paper, we estimate the core radii of our models by fitting King profiles to them in the same manner as in Da Costa et al. (2009). Thus, our quoted core radii can be compared directly to that of Scl-dE1 GC1 reported in that paper.**

By means of numerical simulations we want to investigate whether (1) this EGC could have formed in a DM halo of its own (a scenario in which all globular clusters may reside in their own DM halo was proposed by Mashchenko & Sills (2005)); (2) this EGC could be the product of the merging of two (or more) star clusters. We combine these two scenarios and simulate the merger of two star clusters orbiting in a DM halo. A similar scenario has been proposed by Assmann et al. (2010) as a possible formation mechanism for the luminous components of dwarf galaxies such as dSphs.

In Section 2 we describe the setup of our simulations in detail. In Section 3 we present and discuss our main results, namely that no additional DM is needed to explain the properties of GC1. Finally, in Section 4 we summarise our conclusions.

## 2 SETUP

Initially, we place two star clusters at a distance of 0.5 kpc from each other, at  $x = \pm 0.25$  kpc. While this choice is arbitrary, it ensures that the two clusters are well-separated at the beginning of our simulations. Each star cluster is represented by a Plummer sphere with a Plummer radius (effective radius) of 11 pc and is initially truncated beyond a cut-off radius of 44 pc, **because less than two per cent of the cluster mass resides beyond this radius.** The clusters begin the simulations in equilibrium, but we then mimic the effect of early gas expulsion by artificially reducing the mass of the individual star particles during the first crossing time of the star cluster (10 Myr). **This mass-loss represents not only the loss of gas which has not formed stars, but also mass-loss from the rapid evolution of massive stars, although we note that we do not use a sophisticated mass-loss algorithm as in Dabringhausen et al. (2010), and in the subsequent evolution we do not take mass-loss due to stellar evolution into account. The possible impact of mass-loss from stars on the late-time evolution of a merger remnant at the centre of a dark matter potential well is itself an interesting issue to be explored elsewhere.**

The initial mass of the star clusters is varied according to the adopted star formation efficiency (SFE) in order to obtain final masses (after gas expulsion) of  $2.5 \times 10^4$   $M_\odot$  in all simulations. We consider three values for the SFE, namely 10, 33 and 100 per cent which lead to initial masses of our star clusters of  $2.5 \times 10^5$ ,  $7.6 \times 10^4$  and  $2.5 \times 10^4$   $M_\odot$ , respectively. Each cluster is represented by  $10^5$  particles.

Our model clusters are placed inside spherical DM haloes of different masses and density profiles. **As we are primarily interested in the early evolution of the merger remnant, we treat the halo as an isolated DM halo, ie. we do not simulate the dark matter halo of the dwarf elliptical galaxy Scl-dE1 (Sc22).** We use either a cored Plummer profile (Plummer 1911; Aarseth et al. 1974) with a scale length of 500 pc or a cusped NFW profile (Navarro, Frenk & White 1997; Dehnen & McLaughlin 2005) with a characteristic radius of 500 pc. The mass of the halo enclosed within 500 pc ( $M_{DM}$ ) is varied over many orders of magnitude namely: none,  $5.6 \times 10^4$ ,  $5.6 \times 10^5$ ,  $5.6 \times 10^6$ ,  $5.6 \times 10^7$  and  $5.6 \times 10^8$   $M_\odot$ . The halo is modeled using 1,000,000 particles. As a cut-off radius for our halo we take 2.5 kpc in the Plummer cases and the virial radius for the NFW profiles. Due to the restrictions of fixed scale-length and fixed enclosed mass, the concentrations of our NFW models vary from 2.1 up to 89.5. In Table 1, we give an overview of the main parameters of the dark matter haloes we choose.

In the case of the very low mass halo ( $5.6 \times 10^4$   $M_\odot$ ) we also

**Table 1.** Initial parameters of the dark matter haloes used. The first column denotes the halo profile, which is either Plummer (P) or NFW (N). The second column gives the mass enclosed within 500 pc. In the third column we give the scale length of the halo, either the Plummer radius or the scale radius of the NFW profile. The fourth column gives the cut-off radius of the halo which is chosen to be either  $5 R_{\text{pl}}$  or the virial radius of the NFW halo. Finally, the last column denotes the circular speed of the halo at the initial position of the star clusters.

P/N	$M_{\text{DM}}$ [ $M_{\odot}$ ]	$r_s$ [kpc]	$r_c$ [kpc]	$v_c(250 \text{ pc})$ [ $\text{km s}^{-1}$ ]
P	$5.6 \times 10^4$	0.50	2.50	0.17
N	$5.6 \times 10^4$	0.50	1.05	0.60
P	$5.6 \times 10^5$	0.50	2.50	0.55
N	$5.6 \times 10^5$	0.50	3.03	1.90
P	$5.6 \times 10^6$	0.50	2.50	1.75
N	$5.6 \times 10^6$	0.50	7.81	6.00
P	$5.6 \times 10^7$	0.50	2.50	5.52
N	$5.6 \times 10^7$	0.50	18.98	18.97
P	$5.6 \times 10^8$	0.50	2.50	17.45
N	$5.6 \times 10^8$	0.50	44.73	59.98

**Table 2.** Initial relative velocities of the star clusters in  $\text{km s}^{-1}$ .

case	$v_x$	$v_y$	$v_z$
1	0.00	0.00	0.00
2	0.00	$\pm 0.10$	0.00
3	0.00	$\pm 0.25$	0.00
4	$\pm 0.25$	0.00	0.00

consider different initial relative velocities for the star clusters. The velocities are shown in Table. 2. In the first case the clusters are initially at rest. In the second and third case they have transverse velocities, while in the last case, they have velocities directed towards each other. The choice of velocities is arbitrary, but we show later that our results, to first order, do not depend strongly on this choice of the initial velocities.

We also perform a different set of simulations where we use an initial model for the two star clusters which has a scale-radius (Plummer-radius) of only 4 pc. This is a more standard value for young star clusters (see e.g. Whitmore et al. 1999, and many more).

Finally, we show a suite of simulations in which we place a single star cluster in the centre of the halo and follow its evolution, without a merger, due to the expansion produced by a low SFE.

To perform our simulations we use the particle-mesh code SUPERBOX (Fellhauer et al. 2000). This code has many advantages. One of them is that we can use an arbitrarily high number of particles to model the cluster and the dark matter. **Two-body effects are suppressed in a code of this type and only the smoothed potential is taken into account. Assuming that the simulation results in a merged object which resides in the centre of the DM halo, thereby having a large relaxation-time (of order a Hubble time or longer), this is an appropriate approximation since we would expect that binary formation and two-body encounter would have only a minor effect on our results.**

Another advantage is that SUPERBOX allows us to set different levels of resolution for the different levels of high-resolution grids used in the code. Therefore the code provides the correct resolution in the places where it is most needed. For our models, we use resolutions in the highest resolution grid of 16 pc for the DM halo and 0.4 pc for the star clusters. This means that the internal forces

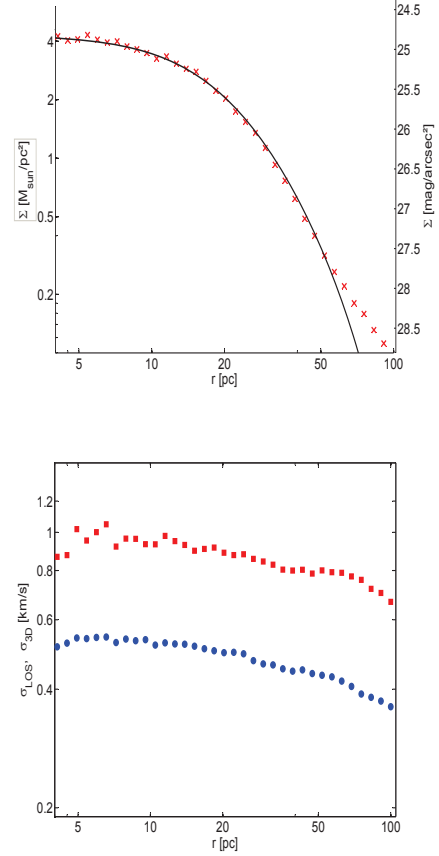


**Figure 1.** Plots showing the properties of the remnant resulting from a cluster merger within a low mass cusped (NFW) DM halo of mass  $M_{\text{DM}} = 5.6 \times 10^4 [M_{\odot}]$  and SFE for the star clusters of 33% (see Table 4). The surface density profile of the EGC is shown in the top panel. The (red online) crosses are the data points, and the solid curve is the King profile fit. It has a core radius  $r_c = 21.5$  pc and a tidal radius  $r_t = 196$  pc. In the bottom panel the velocity dispersions are shown. The (blue online) circles are the line-of-sight velocity dispersion and the (red online) squares are the 3D-velocity dispersion.

within a star cluster, the forces between the two star clusters when they interact and the forces from the star clusters acting on the halo have very high resolution, and the overall force of the background potential of the halo has sufficient resolution to resolve the orbits of the star clusters and the tidal forces acting on them, while keeping computational costs low.

In this code, two-body effects, like binary formation and two-body relaxation are neglected, since they do not play an important role if the final object resides in a DM potential.

### 3 RESULTS

#### 3.1 Cluster merger without DM

The first simulations we perform are of two star clusters which merge under their own gravity without a DM halo present. In Table 3 we show the properties of the merger object after 10 Gyr of evolution. This long time-span is chosen to ensure that the object

**Table 3.** Properties of the merger objects in the no-DM simulations. The first column gives the SFE. The second, third and fourth columns show the parameters of a King profile fit to the resulting merger object, namely the core radius  $r_c$ , the tidal radius  $r_t$  and the central surface brightness  $\mu_0$  assuming a stellar mass to light ratio of 1.0. This choice is arbitrary, because the real value is unknown, but in agreement with visual M/L ratios of many old globulars (e.g. Harris 1996).

SFE [%]	$r_c$ [pc]	$r_t$ [pc]	$\mu_0$ [mag arcsec <sup>-2</sup> ]
100	7	50.1	21.3
33		dissolved	
10		dissolved	

has had time enough to virialize and evolve slowly. We fit King profiles (King 1962) to the final merger objects for this and all models studied because these profiles are widely used in observational astronomy and, in particular, were used in the discovery paper of EGC Scl-dE GC1 (Da Costa et al. 2009). In reality, we would not expect a merger remnant to exhibit a profile with a sharp tidal truncation radius, as in a King profile. Therefore the nominal value of the King tidal radius should be regarded more as a third parameter of the fit rather than a physical property of the remnant.

In the SFE= 100 % case, the fit gives a core radius  $r_c = 7$  pc. This is obviously a smaller value than the initial Plummer radius but this does not imply that the final merger object is denser than its two constituents. Fitting a Plummer profile to the merger object gives a fitted Plummer radius of about 11 pc. So the apparent reduction in  $r_c$  only arises due to the different physical meaning of the scale radius in the two profiles (King and Plummer).

If we introduce super-virial, expanding systems by increasing the initial virial mass of the star cluster (which then gets artificially reduced over one crossing-time), thereby mimicking a lower SFE efficiency of only 33 % (or 10 % respectively) and the expansion due to the gas-expulsion, we do not find a merger object at all. The two star clusters simply disperse and build a very extended distribution of stars, which in the presence of an external host galaxy would have no chance to survive.

### 3.2 Cluster merger with DM

We now place both star clusters in a common, very low-mass DM halo ( $M_{DM} = 5.6 \times 10^4 M_\odot$ ) and test for the influence of the encounter geometry. The results of these simulations are given in Table 4. For the SFE= 100 % cases, the core radii of the resulting EGCs are independent of the initial relative velocities of the clusters, with Plummer profiles yielding EGCs with  $r_c = 7$  pc while NFW haloes lead to more compact EGCs with  $r_c = 3.5$  pc. We find two simulations, using NFW haloes, in which the SCs do not merge and remain as two independent structures. These are the cases in which we give the star clusters transverse velocities of the order of the halo circular velocity. In those cases the star clusters meet off-centre but are compact enough not to merge. This only happens in the NFW models because here the cusp ensures that the orbits of both clusters never lead to close encounters between the clusters. Because of the low mass of the halo and the low densities in the outer regions of the two clusters (we use steep Plummer profiles as initial models), dynamical friction is not strong enough to bring both clusters close enough to merge. However, EGCs always form if the SFE is 33 %. Two of these simulations, which have a Plummer DM halo, result in EGCs with  $r_c = 22$  pc. The EGC formed

**Table 4.** Results of the simulations of cluster mergers in low mass haloes. In all cases, the mass of the halo (enclosed within 500 pc) is  $5.6 \times 10^4 [M_\odot]$ . The first three columns indicate the profile of the DM halo (P for a Plummer profile, N for a NFW profile), the choice of initial cluster relative velocities (with notation according to Table 2), and the adopted SFE. Columns four to six show the parameters of the fitted King profile to the final merger object (i.e. core radius  $r_c$ , half-light radius  $r_h$  (for the fitted King profile), tidal radius  $r_t$  and central surface brightness  $\mu_0$ ), while the seventh column gives the ratio of DM to luminous matter within the central 50 pc of the object. This can be transformed into a regular M/L ratio by adding the masses of both components and adopting a stellar M/L ratio for the luminous component. For example, having a mass-to-mass ratio of unity and adopting a M/L for the luminous component of unity as well, we get a total M/L of 2.

profile P/N	velocity case	SFE [%]	$r_c$ [pc]	$r_h$ [pc]	$r_t$ [pc]	$\mu_0$ [mag/ arcsec <sup>2</sup> ]	$\frac{M_{DM}}{M_{star}}$
P	1	100	7	16.9	45	21.4	0.01
N	1	100	3.5	11.1	31	29.4	0.01
P	1	33	14	39.4	108	23.3	0.01
N	1	33	24	50.9	132	24.5	0.039
P	1	10			dissolved		
N	1	10			dissolved		
P	2	100	7	18.5	50	21.5	0.6
N	2	100			did not merge		
P	2	33	15	35.4	94	23.3	0.13
N	2	33	21.5	69.7	196	24.6	0.036
P	2	10			dissolved		
N	2	10			dissolved		
P	3	100	7	19.7	54	21.6	0.06
N	3	100			did not merge		
P	3	33	22	58.9	160	24.9	0.16
N	3	33	26	53.9	139	24.6	0.02
P	3	10			dissolved		
N	3	10			dissolved		
P	4	100	7	23.4	66	21	0.01
N	4	100	3.5	12.9	37	19.4	0.01
P	4	33	22	64.1	177	24.9	0.16
N	4	33	21	41.5	106	24.6	0.13
P	4	10			dissolved		
N	4	10			dissolved		

inside a NFW DM halo which most closely resembles the properties of Scl-dE GC1 is formed when the relative velocities have a small transversal component (case 2 in Table 2), i.e. the two star clusters do not merge in a head-on collision. In the top panel of Figure 1 we show the surface density profile of this cluster.

It is interesting to note that in all cases with a low SFE of 10 %, we do not form a merger object at all but the two clusters instead dissolve more quickly than they are able to merge. The result is a system with a diffuse light distribution, more similar to a dSph galaxy than a star cluster. In Assmann et al. (2010) and Assmann et al. (in prep.), we explore this scenario for the formation of dSphs in detail.

In Figure 2, we show in the top-left panel the resulting core radii as function of initial cluster relative velocity (see Table 2). It shows clearly that the size of the merger object depends mainly on the adopted SFE and not on the geometry of the first encounter, as long as the two clusters are able to merge. We find no significant general trend in our simulations. As a minimal, second order trend we see, that if the star clusters meet slightly off-centre (velocity cases 2+3) the resulting core radii are mostly slightly larger and if



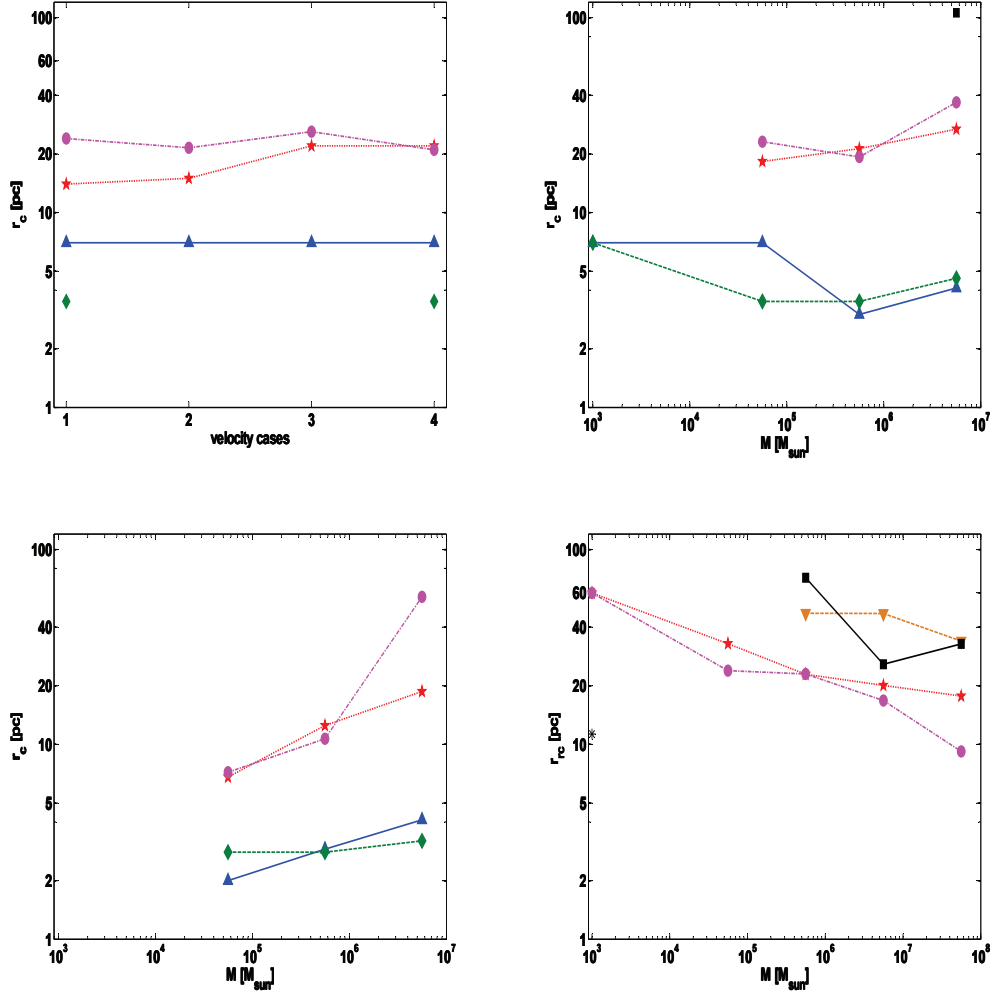


**Figure 2.** **Top-left:** Core radius of our merger objects as function of the adopted relative velocity case (see Table 2). The halo mass was  $5.6 \times 10^4 M_{\odot}$  in all cases. Triangles (blue online) show Plummer profiles and diamonds (green online) show NFW profiles for the halo with a SFE of 100 % for the two star clusters. Stars (red online) and points (magenta online) show Plummer and NFW shapes for the halo, respectively, if the SFE is 33 %. **Top-right:** The core radii of our merger objects as function of the mass of the halo. Triangles (blue online) show Plummer haloes and star clusters with 100 % SFE. Diamond (green online) the same SFE but with NFW haloes. Stars (red online) show Plummer haloes using 33 % for the SFE and points (magenta online) the corresponding NFW cases. The results for the simulations without DM are for comparison shown at a halo mass of 1000 because of the logarithmic scale. The only resulting merger object at a SFE of 10 inside a NFW halo is shown as the square (black online). **Bottom-left:** Core radius versus halo mass for our models with compact star clusters. Triangles (blue) and Diamonds (green) show star clusters with 100 % SFE in haloes with Plummer and NFW profiles, respectively. Stars (red online) show Plummer type haloes and a star cluster with a SFE of 33 %. Circles (magenta) show the same for haloes with NFW profiles. **Bottom-right:** Core radius versus halo mass for our single star cluster models. Stars (red online) show Plummer type haloes and a star cluster with a SFE of 33 %. Points (magenta) show the same for haloes with NFW profiles. Square (black) and Triangles down (orange) show star clusters with 10 % SFE in haloes with Plummer and NFW profile, respectively. Black asterisk show the resulted star cluster from initial compact star cluster evolved without dark matter halo. See text for a detailed discussion.

we increase the speed of the head-on encounter (case 4) we get in most of the cases a smaller core radius.

As a next step, we increase the mass of the halo by factors of 10. The results of our simulations are given in Table 5. Again if the SFE is 100 % we only obtain merger objects with core radii of only  $r_c = 3-7$  pc independent of the mass of the halo. As soon as the SFE is 33 %, it is possible to obtain an EGC which resembles Scl-dE1 GC1 as long as the halo does not become too massive, i.e. the DM content within the final merger object is well below its luminous mass. However, it is interesting to note that in the two cases with  $M_h = 5.6 \times 10^5 M_{\odot}$  the EGCs have a concentration

( $c \equiv \log 10(r_t/r_c)$ ) that is double the estimated concentration of 0.65 for EGC Scl-dE GC1 reported by (Da Costa et al. 2009).

If we consider a mass for the DM halo of  $M_h = 5.6 \times 10^6 M_{\odot}$  and a SFE of 33%, the simulated EGCs have core radii which are too large ( $r_c = 26 - 39$  pc). In other words when the DM content within the merger object is of the same order as that of the luminous matter (mass ratio of 1.7) or significantly higher (mass ratio of 24.4) we get merger objects which are too extended. However, in those cases it may be possible to find a matching model by tuning the SFE to higher values. In almost all simulations with a SFE of 10 %, the SCs dissolve before they merge.

**Table 5.** Results of our simulations for different halo masses (enclosed within a radius of 500 pc). The first column gives the shape of the halo (- for none, P for Plummer and N for NFW), the second column the mass of the halo and the third the SFE. The fourth, fifth and sixth columns give the parameters of a King-profile fitted to the data, namely the core radius, tidal radius and central surface brightness. The last column gives the mass ratio between the DM and the luminous matter within the central 50 pc. The results shown are mean values from up to four different realisations.

profile P/N	$M_h$ [ $M_\odot$ ]	SFE [%]	$r_c$ [pc]	$r_h$ [pc]	$r_t$ [pc]	$\mu_0$ [mag/ arcsec <sup>2</sup> ]	$\frac{M_{DM}}{M_{star}}$
-	0.0	100	7.0	18.5	50.1	21.3	0.0
-	0.0	33			dissolved		
P	$5.6 \times 10^4$	100	7.0	18.4	49.7	21.5	0.025
N	$5.6 \times 10^4$	100	3.5	11.1	31.0	29.4	0.01
P	$5.6 \times 10^4$	33	18.3	49.6	135.0	24.1	0.01
N	$5.6 \times 10^4$	33	23.1	54.0	143.0	24.6	0.06
P	$5.6 \times 10^4$	10			dissolved		
N	$5.6 \times 10^4$	10			dissolved		
P	$5.6 \times 10^5$	100	3.0	11.0	31.5	19.6	0.1
N	$5.6 \times 10^5$	100	3.5	12.3	35.2	19.6	0.13
P	$5.6 \times 10^5$	33	21.3	85.6	249.0	24.4	0.31
N	$5.6 \times 10^5$	33	19.3	103.7	313.0	24.7	0.06
P	$5.6 \times 10^5$	10			dissolved		
N	$5.6 \times 10^5$	10			dissolved		
P	$5.6 \times 10^6$	100	4.1	9.5	25.2	21.1	1.06
N	$5.6 \times 10^6$	100	4.6	29.6	91.0	20.8	3.37
P	$5.6 \times 10^6$	33	26.8	45.4	112.0	23.6	1.69
N	$5.6 \times 10^6$	33	36.8	596	1950	25.8	24.4
P	$5.6 \times 10^6$	10			dissolved		
N	$5.6 \times 10^6$	10	106	198	500	26.0	40.8
P/N	$5.6 \times 10^7$				all simulations dissolve		
P/N	$5.6 \times 10^8$				all simulations dissolve		

Simulations using a higher mass for the DM halo ( $5.6 \times 10^7$  [ $M_\odot$ ] and  $5.6 \times 10^8$  [ $M_\odot$ ] enclosed within 500 pc), lead to completely dissolved star clusters independent of the SFE used. In none of these simulations did we actually see the merging of the two clusters. This can be understood using the theory developed in Fellhauer et al. (2009). If the strength of the background potential becomes too high, i.e. the star clusters meet each other with relative velocities much higher than their internal dispersions it results in destructive high-speed encounters rather than in low velocity merging.

In the top-right panel of Figure 2 we plot the core radius of our merger objects as function of the halo mass. We clearly see that the mass of the halo has only a small influence on the final core radius of the resulting merger object, except for the fact that we have no merger object in very high mass haloes. The main parameter which governs the results is clearly the SFE of the two star clusters. This SFE has to be of order 33 % to obtain a merger object which resembles the EGC.

Da Costa et al. (2009) discussed whether the EGC Scl-dE GC1 could be a dark matter dominated object. Our most important result is that we only get objects which resemble this EGC if the mass of the DM halo within the final stellar distribution is negligible. Higher halo masses lead either to objects which are too extended (i.e. we have to use higher SFEs to counteract external destruction) or to no merged objects at all. **To understand this be-**

**Table 6.** The central line-of-sight velocity dispersions of our best-fitting models, i.e. whose  $r_c$  is close to that of Scl-dE GC1. All cases shown here have a SFE of 33 %. For a halo mass of  $5.6 \times 10^4 M_\odot$  column three gives the velocity case, while for halo masses of  $5.6 \times 10^5 M_\odot$  we give the realisation number.

$M_{halo}$ [ $M_\odot$ ]	profile P/N	velocity case	$r_c$ pc	$\sigma_{LOS,mean}$ km s <sup>-1</sup>
$5.6 \times 10^4$	N	2	21.5	0.78
$5.6 \times 10^4$	P	3	22	0.94
$5.6 \times 10^4$	P	4	22	1.17
$5.6 \times 10^4$	N	4	21	1.68
$5.6 \times 10^5$	P	1	21.4	1.63
$5.6 \times 10^5$	P	2	23	1.66
$5.6 \times 10^5$	N	2	19.5	1.66
$5.6 \times 10^5$	P	3	19.6	1.65
$5.6 \times 10^5$	N	3	19.5	1.62
$5.6 \times 10^5$	P	4	21	1.64
$5.6 \times 10^5$	N	4	20	1.61

havior we need to consider all the competing processes which drive the evolution of the merging clusters within the DM halo. First, it is important to observe that the expansion of the star clusters is governed by the SFE, such that lower SFEs give more extended objects (Baumgardt et al. 2007). Secondly, it must be emphasized that the influences of the DM halo can be divided into two distinct processes, that depend on where the SCs are initially located. One process is when the star clusters have not yet merged in the centre of the DM halo. In this case, the tidal forces generated by DM halo act as an additional destructive force on the clusters, reducing their masses and sizes. The more massive the DM halo, the more dominant is this disruptive process. Additionally, a higher halo mass increases the final relative velocities with which the SCs meet and might, therefore, inhibit the merging. This first halo process tends to lead to remnants which are more extended and diffuse than observed EGCs. The second halo process takes place when the merged object forms and remains at rest in the centre of the DM halo. In this case, the potential well of the DM halo contributes to the gravitational field in which the cluster stars move. As a result, objects which might otherwise dissolve are bound by the DM halo, and the additional gravitational field makes the remnants more compact than they would be without the presence of DM.

Our simulations suggest that mass-to-light ratios of only a few would be expected if the object is formed by the merger of two star clusters, and thus, they are consistent with there being no dynamically significant amount of DM within the stellar distribution of the EGC. However, our results also show that we do require some DM to ensure that the clusters merge to produce an EGC-like remnant, so that DM is an essential part of the merger scenario per se despite not being a significant component of the merger remnant.

In addition to comparing the core radius and concentration of our merger remnants with those of EGC Scl-dE GC1, we can also use our simulations to look at the velocity space of the EGC. Table 6 shows the mean, central line-of-sight velocity dispersion ( $\sigma_{LOS,mean}$ ) for the simulations which resemble the EGC. We average the central dispersion measured along all three coordinates axes (the two coordinates which span the plane of the interaction and the one perpendicular to that) because the orientation of the sight-line towards GC1 relative to any proposed merger is, of course, unknown. In our models,  $\sigma_{LOS,mean}$  varies from 0.78 km s<sup>-1</sup> to 1.68 km s<sup>-1</sup>. In Figure 1 we show the dispersion profile for one

**Table 7.** Results of our simulations for star clusters which are initially more concentrated, i.e. have a Plummer radius of 4 pc. The columns are the same as in Table 5.

profile P/N	$M_{\text{halo}}$ [ $M_{\odot}$ ]	SFE [%]	$r_c$ [pc]	$r_h$ [pc]	$r_t$ [pc]	$\mu_0$ [mag/ arcsec <sup>2</sup> ]	$\frac{M_{\text{DM}}}{M_{\text{star}}}$
—	—	100			did not merge		
—	—	33			did not merge		
P	$5.6 \times 10^4$	100	2	25.1	81	19.2	0.03
N	$5.6 \times 10^4$	100	2.8	12.5	37	19.1	0.01
P	$5.6 \times 10^4$	33	6.8	12.1	30.3	22.05	0.06
N	$5.6 \times 10^4$	33	7.2	24.1	68.2	22.0	0.02
P	$5.6 \times 10^4$	10			dissolved		
N	$5.6 \times 10^4$	10			dissolved		
P	$5.6 \times 10^5$	100	2.9	9.9	28	19.3	0.13
N	$5.6 \times 10^5$	100	2.8	14.0	42	19.4	0.2
P	$5.6 \times 10^5$	33	12.5	—	$1.2e+5$	24.2	0.35
N	$5.6 \times 10^5$	33	10.7	—	$1.2e+3$	23.9	0.7
P	$5.6 \times 10^5$	10			did not merge		
N	$5.6 \times 10^5$	10			dissolved		
P	$5.6 \times 10^6$	100	4.1	10.4	28	21.88	1.1
N	$5.6 \times 10^6$	100	3.2	33.2	106	20.33	3.34
P	$5.6 \times 10^6$	33	18.7	—	$3.1e+4$	24.5	0.35
N	$5.6 \times 10^6$	33	57.2	—	$1.2e+5$	26.1	24.1
P	$5.6 \times 10^6$	10			dissolved		
N	$5.6 \times 10^6$	10			dissolved		

of our merger objects. It is notable that it is possible to increase the central dispersion of our merger object up to almost  $1.7 \text{ km s}^{-1}$  without having significant amounts of DM within the object.

The importance of studying the velocity space of the simulated clusters is that the velocity dispersions can be used to distinguish between our various scenarios for the formation of EGC Scl-dE GC1. Moreover, the velocities obtained in our simulations can be compared with future observations to infer the presence or absence of dark matter in the system.

### 3.3 Compact initial clusters

For comparison, we also perform simulations with a more standard model for the initial star cluster, i.e. with a Plummer radius of just 4 pc. With this suite of simulations we want to investigate whether it is possible to obtain EGCs like GC1 without starting with star clusters that are already extended.

The results in Table 7 and the bottom-left panel of Figure 2, show clearly that we do not end up with a merger object that resembles the properties of GC1, if the initial star clusters are too concentrated. A SFE which guarantees the survival of the two clusters always leads to merged objects which are too concentrated to resemble the EGC in Sculptor. All our merged objects show core radii of less than or about 10 pc. This behavior is explained by the force performed by the DM halo as soon as the merger SCs are settled in the centre. This force keeps the merged object together and more compact. The exceptions are the simulations with a  $5.6 \times 10^6 M_{\odot}$  halo. Here again we see a completely dissolved object but this time it is possible to determine a centre of density. However, even though the fitted 'core radii' seem to match the properties of the EGC, one sees from the values of the 'tidal radii' that these are not really EGCs but rather fluffy, low-density distributions of stars. Taking these results

**Table 8.** Results of our simulations with a single star cluster expanding because of mass-loss due to gas-expulsion. The columns are the same as in Table 5. For the non-DM simulations we give two simulations which have a SFE of 33 %. The first simulation started with a more compact Plummer sphere and has a Plummer radius of 4 pc, while the second one shows the standard 11 pc model.

profile P/N	$M_h$ [ $M_{\odot}$ ]	SFE [%]	$r_c$ [pc]	$r_h$ [pc]	$r_t$ [pc]	$\mu_0$ [mag/ arcsec <sup>2</sup> ]	$\frac{M_{\text{DM}}}{M_{\text{star}}}$
-	0.0	33	11.3	21.1	53.4	24	—
-	0.0	33	59.9	62.7	139	27.6	—
-	0.0	10			dissolved		
P	$5.6 \times 10^4$	33	32.9	34.5	76.5	23.6	0.23
N	$5.6 \times 10^4$	33	23.9	42.3	105.6	24.2	0.03
P	$5.6 \times 10^4$	10			dissolved		
N	$5.6 \times 10^4$	10			dissolved		
P	$5.6 \times 10^5$	33	22.9	39.2	97.2	23.7	0.21
N	$5.6 \times 10^5$	33	23	34.3	82.3	23.3	0.35
P	$5.6 \times 10^5$	10	47.1	84.0	210	26.3	0.55
N	$5.6 \times 10^5$	10	71.7	67.7	147	25.7	0.5
P	$5.6 \times 10^6$	33	20.1	37.9	96	23.1	0.8
N	$5.6 \times 10^6$	33	16.8	29.1	72.2	22.5	4.1
P	$5.6 \times 10^6$	10	47	51.4	115	24.1	1.34
N	$5.6 \times 10^6$	10	25.8	86.0	243	24.1	4.2
P	$5.6 \times 10^7$	33	17.7	29.6	73	22.5	5.89
N	$5.6 \times 10^7$	33	9.2	—	$3.5e+4$	23.8	74.8
P	$5.6 \times 10^7$	10	33.9	36.3	81	23.01	7.78
N	$5.6 \times 10^7$	10	32.8	—	$4.7e+5$	25.34	91.2

into account we can rule out that the EGC has formed out of two concentrated star clusters.

### 3.4 Abandoning the merger scenario

To complete our survey of possible formation scenarios we now abandon the hypothesis that Scl-dE1 GC1 formed via a merger of multiple clusters and explore whether it is possible to expand a single young star cluster sufficiently due to gas-expulsion to resemble the observed EGC.

Our simulations (results are shown in Table 8) show clearly that it is possible to get an extended star cluster just by expansion due to gas-expulsion alone. In our simulations we do not include any tidal field of the parent galaxy and therefore our star cluster can expand freely without fearing destruction due to external tidal forces. In the case without DM, we use only our standard SFE of 33 %, which has been shown in many studies (e.g. Baumgardt et al. 2007) to be the lowest limit for a cluster to survive gas-expulsion. Therefore it is no wonder that the cluster expands significantly. However, by using higher SFE and/or initially more compact clusters it is likely that we could find a suitable model to reproduce the observed data. **We performed one simulation which started from a compact star cluster with a Plummer radius of only 4 pc and was transformed into an EGC with a scale length of 11.3 pc, while a cluster with an initial Plummer radius of 11 pc was transformed into an EGC with a scalelength of  $\sim 60$  pc. This clearly shows that we would be able to get a model which reproduces the observed data by using an intermediate initial scale-length.** Applying Occam's Razor, this might be the simplest and most plausible way to explain the origin of the EGC in Sculptor. However, the intention

**Table 9.** The central line-of-sight velocity dispersion of our best-fitting, single-cluster models, i.e. whose  $r_c$  is close to the one of Scl-dE GC1. All cases shown here have a SFE of 33 %. **In the first two lines we give the results obtained in our non-DM simulations. The values of  $r_c$  in these models bracket that of the observed EGC - as discussed in the text, we expect that a good model of the observed data could be obtained for an intermediate value of the initial cluster Plummer radius.**

$M_{\text{halo}}$ [ $M_{\odot}$ ]	profile P/N	$r_c$ pc	$\sigma_{\text{LOS,mean}}$ km s $^{-1}$
0	—	11.3	1.08
0	—	59.9	0.18
$5.6 \times 10^4$	N	23.9	1.06
$5.6 \times 10^5$	N	23	1.73
$5.6 \times 10^5$	P	22.9	1.66
$5.6 \times 10^6$	P	20.1	2.27

of this paper is mainly to test and investigate the alternative, and more complicated, formation scenarios which have been proposed in the literature.

If we place the single cluster in the centre of its own DM halo, we first see that the more massive the halo gets the more likely it is for the star cluster to survive even for SFEs as low as 10 %. The higher the halo mass the more gravitational potential there is to halt the expansion and therefore the more compact our resulting object is. This trend is visible in the bottom-right panel of Figure 2. With our initial cluster model and values for the SFE we get the best matches for intermediate mass haloes of  $5.6 \times 10^4$  to  $5.6 \times 10^6 M_{\odot}$  for both kinds of halo profile. Again we see no significant trend with halo profile except that we expect the NFW haloes to have more mass in the region of interest than the equivalent Plummer model. However, from the general behavior of our results we expect to be able to find a suitable solution for any halo mass. If we had extended our parameter space to include even more massive haloes then we would likely have obtained a match even for SFE of 10 %. At lower halo masses we could use either initially more compact clusters or assume higher SFEs.

Finally in Table 9 we show the LOS velocity dispersion of our best-fitting, single-cluster models. As expected, the central velocity dispersion rises with DM halo mass, from below one km s $^{-1}$  for the non-DM case up to more than two km s $^{-1}$  for the DM dominated one, and therefore will be the crucial parameter to decide whether or not this very extended object has its own DM halo, once spectroscopic data are available.

#### 4 CONCLUSIONS

In this paper, we explored several of the proposed formation scenarios for the recently-discovered, extended globular cluster GC1 associated with the dwarf elliptical galaxy Scl-dE1 in the Sculptor group of galaxies. Even though extended globular clusters have been found in the haloes of many galaxies, this is the first such object found in orbit around a dwarf galaxy and exhibiting a very large core radius.

There are two obvious scenarios for the formation of an extended stellar system starting from one, or several, individual constituents. The first, and probably more natural, scenario is via the expansion induced by either gas expulsion or stellar mass loss during the early evolution of a normal star cluster. The other viable scenario is that extended objects form via the merger of smaller

systems. A third, more recent proposal for the formation of globular clusters is that they might reside in their own DM halo, thereby helping to solve the missing satellite problem. We have extended those speculations to the object of our study. In this paper, we have combined aspects of these three scenarios in order to investigate thoroughly which initial conditions can lead to an object which resembles the observations.

Taking all our merger simulations into account, we see the following trends:

(i) As expected, for an assumed SFE of 100%, mergers of two clusters without the presence of DM produce a remnant which is of similar density to the original clusters, while lower SFEs lead to the dissolution of both initial clusters without merging. Finely tuned initial conditions would be required to produce a merger remnant via this route which matches Scl-dE1 GC1 in terms of size.

(ii) Mergers of two virialised clusters within a DM halo do not, in general, lead to a remnant which is more extended than the original clusters. This result is independent of the assumed halo mass. We therefore need to invoke additional expansion either due to a SFE which is lower than 100 % or due to mass loss from early stellar evolution to produce extended remnants.

(iii) For high halo masses, we find that low SFEs can lead to the dispersal of the star clusters before they have time to merge. In those cases we see an extended luminous component which more closely resembles a dSph galaxy than a globular cluster. This coincides with the formation theory for dSph galaxies we discuss in Assmann et al. (2010) and Assmann et al. (in prep.).

(iv) In all the simulations which led to an extended remnant whose appearance matched that of Scl-dE1 GC1, the mass of DM enclosed within the volume probed by the stars of the EGC was not sufficient to raise the mass to light ratio significantly above the stellar M/L. Therefore, even though our simulations can not rule out that this extended globular cluster resides in its own DM halo we do not expect it to be a highly DM dominated object at the present day.

(v) We have shown that our models can be tested by future observations. In our remnants, the higher the DM content, the higher is the central velocity dispersion of our merger object ranging from 0.7 to 1.7 km s $^{-1}$ . **The next generation telescopes, for example the Extremely Large Telescope, may be able to measure such differences either from the integrated spectra of the clusters or from observations of individual cluster stars, which can then be compared with the predictions of the models we have simulated.**

(vi) If we merge clusters which are initially as compact as typical globular clusters, we find that it is very difficult to form an object resembling the observed EGC. We need to lower the SFE below the general survival limit while still requiring that the clusters merge in the centre of the halo before they dissolve completely. Such chance mergers are possible and have been found in other studies as well (Fellhauer & Kroupa 2005), but are unlikely to be a dominant formation avenue.

Abandoning the merger scenario, we have shown that we can also form an object like GC1 via the expansion due to gas-expulsion during the formation of the cluster. In these models, we start with an object forming in the very centre of a DM halo and show that gas expulsion produces remnant clusters whose extent depends on the mass of the halo - the higher the halo mass the more compact is the remnant. With high halo masses it is possible to get surviving and matching objects by using SFEs which would lead to the complete dissolution of the cluster in the absence of DM. Starting out with a more compact object leads to a final remnant which is more com-



pact. Thus, for any given halo mass, it is possible to match the data either by changing the SFE or by changing the initial size of the object. Again, as in the merger scenario, the observable difference between the models which resemble Scl-dE1 GC1 is their velocity dispersion. The higher halo mass, and therefore the DM content within the EGC, the higher its velocity dispersion will be.

The velocity dispersions of globular clusters containing Intermediate-Mass Black Holes (IMBH) at their centres have been discussed by Baumgardt et al. (2005) using numerical models. The velocity dispersion for a star cluster of similar stellar mass to our EGC is raised by only  $0.1\text{--}0.5\text{ km s}^{-1}$  in the inner 10 per cent of the half-mass radius. The same would also be true for the stronger effect of a binary IMBH. In both cases, the increase in velocity dispersion is seen only in the core the star cluster. Other numerical simulations show, that even if there is a high binary black hole fraction within a globular cluster (Mackey et al. 2008), the central line of sight velocity dispersion is about  $1.0\text{--}1.5\text{ km s}^{-1}$  about double the value, but shows the regular fall-off at the outer radii as well.

To distinguish between the presence of a black hole and the presence of dark matter distributed within the cluster would require the measurement of the velocity dispersion as a function of radius within the cluster. If the EGCs contain dark matter, then their velocity dispersions will remain higher than expected at large radii, not solely at the centre. For some EGCs, such observations may be feasible with the next generation of extremely large telescopes.

Finally, we note that it is possible to obtain an object like Scl-dE1 GC1 just by using expansion due to mass-loss (gas expulsion and/or stellar winds) within a single young cluster. Fine-tuning the initial concentration of the cluster and, in our case, the SFE leads to an object which matches the data. In the light of Occam's razor this might be the most simplest and straightforward solution to explain the properties of Scl-dE1 GC1. The key test of this model would be the survivability of the remnant in the tidal field of the host galaxy. This would require further simulations of the evolution of the cluster in the external tidal field following the period of expansion and is beyond the scope the present paper.

We conclude that the unusually large size of the extended star cluster Scl-dE1 GC1 does not require the presence of dynamically significant DM in this system. We have shown that there are several formation paths for this object involving mergers of star clusters in low-mass dark matter haloes which result in a remnant that contains very little DM interior to the stellar distribution. It is also possible to form the object through the expansion of a single star cluster as a result of mass loss. Thus, we have demonstrated that the formation scenarios proposed for this system in the literature are plausible. To make further progress requires the measurement of a precise velocity dispersion for the object, as this would enable us to distinguish between formation models which require DM and those which require only baryonic matter. To distinguish between scenarios which involve merging of two or more initial objects and models which only expand due to gas-expulsion alone, one might also be able to look for irregular chemical abundances in the stars of the cluster which could point to an origin in different clusters.

**Acknowledgments:** PA is supported through a CONICYT PhD scholarship and wishes to thank W. Dehnen for his help with the NFW profiles. PA also announces help through the MECESUP travel grant FSM0605. MF acknowledges financial support through FONDECYT grant no. 1095092. MIW acknowledges the Royal Society for support through a University Research Fellowship.

## REFERENCES

- Aarseth S.J., Henon M., Wielen R. 1974, *A&A*, 37, 183  
 Assmann P., Fellhauer M., Wilkinson M.I., 2010, *IAUS*, 266, 353A  
 Baumgardt H., Makino J., Hut P. 2005, *APJ*, 620, 243  
 Baumgardt H. & Kroupa P., 2007, *MNRAS*, 380, 1589  
 Bekki K., Couch W.J., Drinkwater M.J. 2001, *ApJ*, 552, 105  
 Belokurov V., et al. (10 co-authors) 2010, *ApJL*, 712, 103L  
 Brüns R.C., Kroupa P., Fellhauer M. 2009, *ApJ*, 702, 1268  
 Chandar R., Whitmore B., & Lee, M.G. 2004, *ApJ*, 611, 220  
 Dabringhausen J., Fellhauer M., Kroupa P., 2010, *MNRAS*, 403, 1054  
 Da Costa G.S., Grebel E.K., Jerjen H., Rejkuba M., Sharina M.E. 2009, *AJ*, 137, 4361  
 Dehnen W., McLaughlin D.E. 2005, *MNRAS*, 363, 1057  
 Fellhauer M., Kroupa P., Baumgardt H., Bien R., Boily C.M., Spurzem R., Wassmer N., 2000, *New Ast.*, 5, 305  
 Fellhauer M., Kroupa P. 2002, *MNRAS*, 330, 642  
 Fellhauer M., Kroupa P. 2005, *ApJ*, 630, 879  
 Fellhauer M., Wilkinson M.I., Kroupa P. 2009, *MNRAS*, 397, 1268  
 Gilmore G., Wilkinson M.I., Wyse R.F.G., Kleya J.T., Koch A., Evans N.W., Grebel E.K. 2007, *ApJ*, 663, 948  
 Gomez M., & Woodley K.A. 2007, *ApJ*, 670, L105  
 Harris W.E. 1996, *AJ*, 112, 1487  
 Hasegan M., et al. (12 co-authors) 2005, *ApJ*, 627, 203  
 Hurley J. R., 2007, *MNRAS*, 379, 93  
 Huxor A.P., Tanvir N.R., Irwin M.J., Ibata R., Collett J.L., Ferguson A.M.N., Bridges T., Lewis G.F. 2005, *MNRAS*, 360, 1007  
 Huxor A.P., Tanvir N.R., Ferguson A.M.N., Irwin M.J., Ibata R., Bridges T., Lewis G.F. 2008, *MNRAS*, 385, 1989  
 Hwang N., Lee M.G., Lee C.L., Park W-K., Park H.S., Park J-H., Sohn S.T., Lee S-G., Lee H.M., Chun M-S., Lee Y-W., Sohn Y-J., Yuk I-S., Kim S.C., Kim H-I., Han W., 2005, *IAUC.*, 198, 257  
 King, I. 1962, *AJ*, 67, 471  
 Kleya J.T., Wilkinson M.I., Evans N.W., Gilmore G. 2005, *ApJ*, 630, L141  
 Lane R.R., Kiss L.L., Lewis G.F., Ibata R.A., Siebert A., Bedding T.R., Székely P., Balog Z., Szabó G.M. 2010, *MNRAS*, 406, 2732  
 Larson S.S., Brodie J.P. 2000, *AJ*, 120, 2938  
 Mackey A. D., Wilkinson M.I., Davies M.B., Gilmore G.F. 2008, *MNRAS*, 386, 65  
 Mashchenko S., Sills A. 2005, *ApJ*, 619, 243  
 Mateo M. 1998, *ARA&A*, 36, 435  
 Mieske S., Hilker M., Infante L. 2002, *A&A*, 383, 823  
 Navarro J.F., Frank C.S., White S.D.M. 1997, *ApJ*, 490, 493  
 Plummer, H. C., 1911, *MNRAS*, 71, 460  
 Strigari L.E., Koushiappas S.M., Bullock J.S., Kaplinghat M., Simon J.D., Geha M., Willman B. 2008, *ApJ*, 678, 614  
 Walker M.G., Mateo M., Olszewski E.W., Peñarrubia J., Evans N.W., Gilmore G., 2009, *ApJ*, 704, 1274  
 Wilkinson M. I., Hurley J. R., Mackey A. D., Gilmore G. F., Tout C. A., 2003, *MNRAS*, 343, 1025  
 Whitmore B.C., Zhang Q., Leitherer C., Fall S.M., Schweizer F., Miller B.W. 1999, *AJ*, 118, 1551